BNWL-CC-664

MULTI-NODE SIMULATION OF THE FFTF INTERMEDIATE HEAT EXCHANGER

L. H. Gerhardstein
Systems Analysis and Simulation
Computers and Controls Section
Applied Physics and Electronics Department

May 1966

NOTICE: PRELIMINARY REPORT

This report contains information of a preliminary nature prepared in the course of work under Atomic Energy Commission Contract AT-(45-1)-1830. This information is subject to correction or modification upon the collection and evaluation of additional data.

LEGAL NOTICE

PACIFIC NORTHWEST LABORATORY
RICHLAND, WASHINGTON
OPERATED BY
BATTELLE MEMORIAL INSTITUTE
for the
U.S. ATOMIC ENERGY COMMISSION Under Contract No. AT(45-1)-1830.

TABLE OF CONTENTS

	Page
SUMMARY AND CONCLUSIONS	4
MODEL DEVELOPMENT	4
NODAL EQUATIONS	7
SAMPLE RESULTS	10
APPENDIX A	16
Calculation of Heat Exchanger Constants	16
BIBLIOGRAPHY	18
NOMENCLATURE	19

LIST OF FIGURES

Number	Title	Page
1	Pictorial View, Counter Current Heat Exchanger	4
2	Differential Counter Current Heat Exchanger	4
3	Nodalized Heat Exchanger Temperature Profile	8
4	Heat Exchanger Temperature Profile, One Node	11
5	Heat Exchanger Temperature Profile, Two Nodes	12
6	Heat Exchanger Profile, Four Nodes	13
7	Heat Exchanger Profile, Eight Nodes	14
8	FFTF Intermediate Heat Exchanger	15
9	Intermediate Heat Exchanger Tube Geometry	16

MULTI-NODE SIMULATION OF THE FFTF INTERMEDIATE HEAT EXCHANGER

SUMMARY AND CONCLUSIONS

A tube and shell counter flow heat exchanger is used in each primary loop of the FFTF Conceptual Design[1] with liquid sodium as the primary and secondary coolants. A multi-node model of the intermediate heat exchanger (IHX) was developed and is being used in a four node configuration with the FFTF dynamics analog simulation. A series of tests using 1, 2, 4, and 8 nodes for the IHX simulation indicated that a four-node model will adequately represent the process.

MODEL DEVELOPMENT

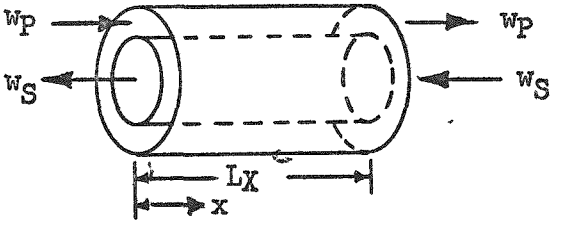

FIGURE 1. Pictorial View, Counter Current Heat Exchanger

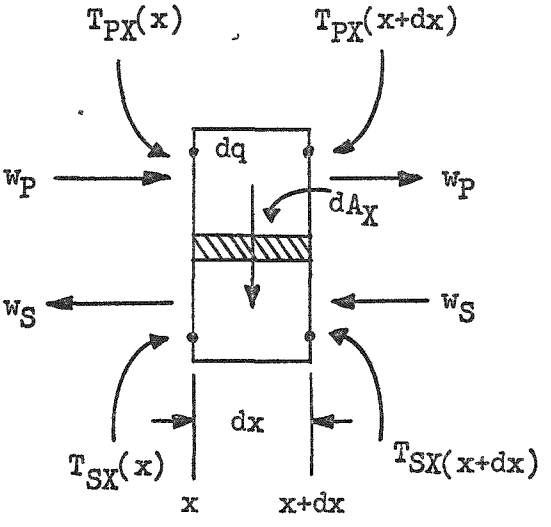

FIGURE 2. Differential Counter Current Heat Exchanger

Figure 1 shows a fundamental view of a single pass counter current heat exchanger. Figure 2 is a heat exchanger slab with length dx, heat transfer area dA, and heat transfer rate dq. The primary inlet and outlet temperatures of the slab are $T_{PX}(x)$ and $T_{PX}(x + dx)$, respectively. Likewise, the secondary inlet and outlet temperatures of the slab are $T_{SX}(x + dx)$ and $T_{SX}(x)$. There is a differential heat capacity-mass product associated with both primary and secondary sides, $d(MC)_{PX}$ and $d(MC)_{SX}$, which take into account both metal and coolant masses and heat capacities. Thus,

$$d(MC)_{PX} = C_{CPX}dM_{CPX} + C_{MPX}dM_{MPX} \tag{1}$$

and

$$d(MC)_{SX} = C_{CSX}dM_{CSX} + C_{MSX}dM_{MSX} \tag{2}$$

where the subscripts C and M refer to coolant and metal, respectively. The differential mass quantities can be written as:

$$dM_{CPX} = A_{CPX}\rho_{CPX}dx \tag{3}$$

$$dM_{CSX} = A_{CSX}\rho_{CSX}dx \tag{4}$$

$$dM_{MPX} = A_{MPX}\rho_{MPX}dx \tag{5}$$

$$dM_{MSX} = A_{MSX}\rho_{MSX}dx \tag{6}$$

The heat storage rates in primary and secondary differential volumes are:

$$d\dot{Q}_P = \dot{Q}_{Pin} - \dot{Q}_{Pout} - dq \tag{7}$$

$$d\dot{Q}_S = \dot{Q}_{Sin} - \dot{Q}_{Sout} + dq \tag{8}$$

where the inlet and outlet heat flow rates are:

$$\dot{Q}_{Pin} = w_P C_{CPX} T_{PX}(x,t) \tag{9}$$

$$\dot{Q}_{Pout} = w_P C_{CPX} T_{PX}(x + dx,t) \tag{10}$$

$$\dot{Q}_{Sin} = w_S C_{CSX} T_{SX}(x + dx,t) \tag{11}$$

$$\dot{Q}_{Sout} = w_S C_{CSX} T_{SX}(x,t) \tag{12}$$

The temperatures at x + dx are:

$$T_{PX}(x + dx,t) = T_{PX}(x,t) + \frac{\partial T_{PX}}{\partial x}dx \tag{13}$$

and

$$T_{SX}(x + dx,t) = T_{SX}(x,t) + \frac{\partial T_{SX}}{\partial x}dx \tag{14}$$

The heat transfer rate is:

$$dq = U_X dA_X \left[T_{PX}(x) - T_{SX}(x) \right] \tag{15}$$

where the differential heat transfer area is

$$dA_X = \frac{dA_X}{dx} dx \quad .$$

For a uniform area distribution,

$$\frac{dA_X}{dx} = \frac{A_X}{L_X}$$

Thus, the differential heat transfer rate is:

$$dq = \frac{U_X A_X}{L_X} \left(T_{PX} - T_{SX} \right) dx \tag{16}$$

The heat storage rates, $d\dot{Q}_P$ and $d\dot{Q}_S$, can also be written as

$$d\dot{Q}_P = d(MC)_{PX} \frac{\partial T_{PX}(x,t)}{\partial t} \tag{17}$$

and

$$d\dot{Q}_S = d(MC)_{SX} \frac{\partial T_{SX}(x,t)}{\partial t} \tag{18}$$

Substituting Equations (9) and (10) into (7); and (11) and (12) into (8) yields:

$$d\dot{Q}_P = w_P C_{CPX} \left[T_{PX}(x,t) - T_{PX}(x + dx, t) \right] - dq$$

and

$$d\dot{Q}_S = w_S C_{CPX} \left[T_{SX}(x + dx, t) - T_{SX}(x,t) \right] + dq$$

Substitution of Equations (13) and (14) yields:

$$d\dot{Q}_P = - w_P C_{CPX} \frac{\partial T_{PX}}{\partial x} dx - dq \tag{19}$$

and

$$d\dot{Q}_S = w_S C_{CSX} \frac{\partial T_{SX}}{\partial x} dx + dq \tag{20}$$

Combination of Equations (1) through (6) and substitution in (17) and (18) yields:

$$d\dot{Q}_P = (A_{CPX}\ \rho_{CPX}\ C_{CPX} + A_{MPX}\ \rho_{MPX}\ C_{MPX}) \frac{\partial T_{PX}}{\partial t} dx \tag{21}$$

and

$$d\dot{Q}_S = (A_{CSX}\ \rho_{CSX}\ C_{CSX} + A_{MSX}\ \rho_{MSX}\ C_{MSX}) \frac{\partial T_{SX}}{\partial t} dx \tag{22}$$

Substituting Equations (16), (21), and (22) into (19) and (20) and cancellation of dx yields:

$$(A_{CPX}\ \rho_{CPX}\ C_{CPX} + A_{MPX}\ \rho_{MPX}\ C_{MPX}) \frac{\partial T_{PX}}{\partial t} =$$

$$- w_P C_{CPX} \frac{\partial T_{PX}}{\partial x} - \frac{U_X A_X}{L_X} \left(T_{PX} - T_{SX}\right) \tag{23}$$

and

$$(A_{CSX}\ \rho_{CSX}\ C_{CSX} + A_{MSX}\ \rho_{MSX}\ C_{MSX}) \frac{\partial T_{SX}}{\partial t} =$$

$$w_S C_{CSX} \frac{\partial T_{SX}}{\partial x} + \frac{U_X A_X}{L_X} \left(T_{PX} - T_{SX}\right) \tag{24}$$

NODAL EQUATIONS

Equations (23) and (24) are the basic partial differential equations for a counter current heat exchanger. The method of finite differences was used to develop a multi-node mathematical model consisting of a set of ordinary differential equations.

Central and backward difference methods were used to develop multi-node models of the IHX. The backward difference method was chosen for use with the FFTF dynamics simulation because certain unrealistic effects associated with central difference simulation of counter current heat exchangers are not present when backward difference is used. This can be demonstrated by referring to Figure 3 and the central difference slope equations for equal spacing:

$$\left.\frac{\partial T_{(K)PX}}{\partial x}\right|_{x_K} = \frac{T_{(K+1)PX} - T_{(K-1)PX}}{2\Delta x}$$

For demonstration purposes assume that secondary flow is low, primary flow is high, and a temperature increase is presented to the secondary inlet $T_{(n_X)SX}$. Primary outlet temperature $T_{(n_X)PX}$ increases quickly due to heat transfer but $T_{(n_X)SX}$ has little immediate effect on $T_{(n_X-1)SX}$ since secondary flow rate is low. Thus, $T_{(n_X-1)PX}$ has little change due to $T_{(n_X-1)SX}$ but is affected by $T_{(n_X)PX}$ since and increase in $T_{(n_X)PX}$ causes the temperature gradient at $T_{(n_X-1)PX}$ to increase. From Equation (23), the result is that $T_{(n_X-1)PX}$ decreases when $T_{(n_X)PX}$ increases. Since the primary coolant at $T_{(n_X)PX}$ is $T_{(n_X)PX}$ is flowing out of the heat exchanger, any effect of $T_{(n_X)PX}$ upon $T_{(n_X-1)PX}$ is unrealistic. The backward difference method does not present these inaccuracies in the simulation and was, therefore, chosen for the FFTF dynamics simulation.

Figure 3 shows the temperature distribution of the primary and secondary sides of the heat exchanger and the relative locations of the nodes.

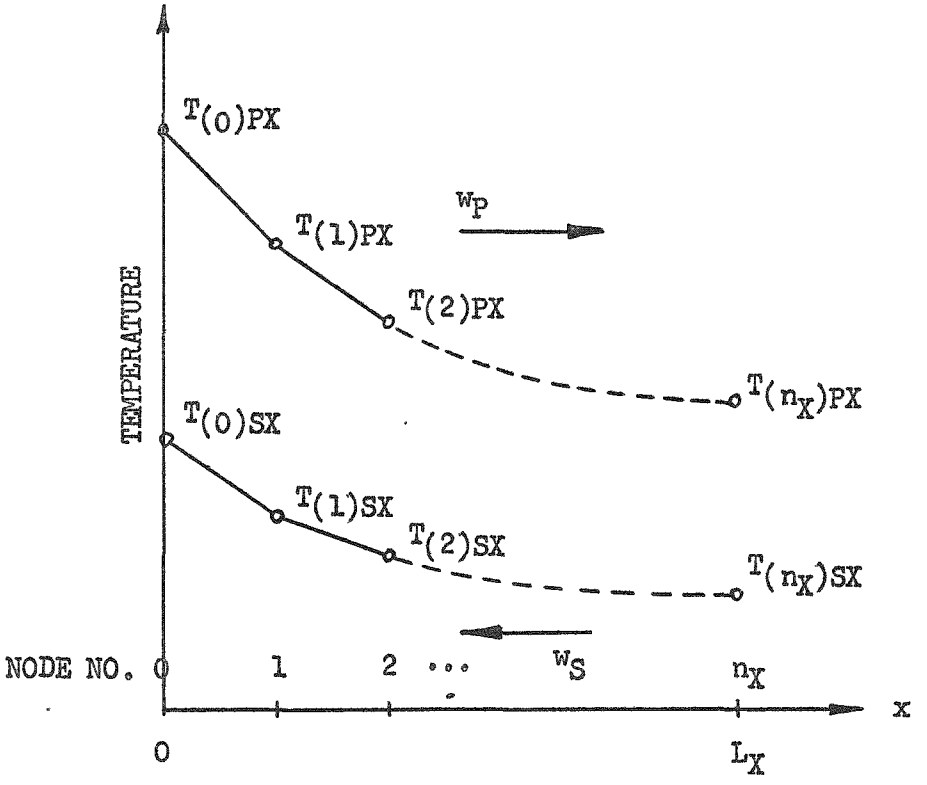

FIGURE 3

Nodalized Heat Exchanger Temperature Profile

The nodes are numbered from zero to n_X (the number of nodes in the heat exchanger model). The primary and secondary inlet temperatures (inputs) are $T_{(o)PX}$ and $T_{(nX)SX}$, respectively. The outlet temperatures are $T_{(nX)PX}$ and $T_{(o)SX}$. The spacing between node K-1 and node K is Δx_{KX}. If a uniform spacing of nodes is to be used, all the Δx_{KX} are L_X/n_X.

Using the backward finite difference method and since primary coolant flow is from the left (Figure 3), the primary temperature gradient at the K^{yh} node is:

$$\left.\frac{\partial T_{PX}}{\partial x}\right|_K = \frac{T_{(K)PX} - T_{(K-1)PX}}{\Delta x_{KX}} \tag{25}$$

Likewise, for the secondary side, since heat flow is from the right, the backward difference method gives:

$$\left.\frac{\partial T_{SX}}{\partial x}\right|_K = \frac{T_{(K+1)SX} - T_{(K)SX}}{\Delta x_{(K+1)X}} \tag{26}$$

The partial derivatives with respect to time reduce to the total derivatives:

$$\left.\frac{\partial T_{PX}}{\partial t}\right|_K = \frac{dT_{(K)PX}}{dt} \tag{27}$$

$$\left.\frac{\partial T_{SX}}{\partial t}\right|_K = \frac{dT_{(K)SX}}{dt} \tag{28}$$

Substituting Equations (25), (26), (27), and (28) into Equations (23) and (24),

$$(A_{CPX}\rho_{CPX}C_{CPX} + A_{MPX}\rho_{MPX}C_{MPX})\frac{dT_{(K)PX}}{dt} =$$

$$\frac{w_P C_{CPX}}{\Delta x_{KX}}(T_{(K-1)PX} - T_{(K)PX}) - \frac{U_X A_X}{L_X}(T_{(K)PX} - T_{(K)SX}) \tag{29}$$

$$(A_{CSX}\rho_{CSX}C_{CSX} + A_{MSX}\rho_{MSX}C_{MSX})\frac{dT_{(K)SX}}{dt} =$$

$$\frac{w_S C_{CSX}}{\Delta x_{(K+1)X}}(T_{(K+1)SX} - T_{(K)SX}) + \frac{U_X A_X}{L_X}(T_{(K)PX} - T_{(K)SX}) \qquad (30)$$

SAMPLE RESULTS

Equations (29) and (30) are used in the FFTF dynamics simulation for representation of the IHX. A series of runs were made using 1, 2, 4, and 8 nodes with aheat exchanger simulation using FFTF IHX parameters.[2] A sample of the temperature profiles obtained as a function of time for the different multi-node cases is shown in Figures 4, 5, 6, and 7. The conditions used for the runs shown were:

w_P and w_S = constant (2270 lb/sec)

$T_{(n_X)SX}$ = constant (575 °F)

$T_{(o)PX}$ = decaying exponential from 975° to 775° with a time constant of one second

Increasing the number of nodes increases transport lag accuracy. This is seen by inspection of the temperature profiles shown in Figures 4 through 7. The four and eight node cases (Figures 6 and 7) show the temperature disturbance is propagated along the length of the primary side of the heat exchanger with respect to both lag time and attenuation of the wave. The wave is not present with one node (Figure 4), and only slightly present with two nodes (Figure 5). Comparison of the 4 and 8 node models shows that little accuracy is gained by using eight nodes. Therefore, four nodes was chosen as the best compromise between accuracy and computer equipment.

The analog simulation diagram of the IHX is shown in Figure 8. A four node model of the IHX is used. Flow rate multiplications are performed by servo-multipliers (not shown on diagram). The simulation has been constructed with constant heat transfer coefficient that represents design conditions (see Appendix). The representation of a variable heat transfer coefficient will be introduced in the simulation as a deviation from design conditions so that the scaling of non-linear equipment can be kept as low as possible. Calculations of the heat exchanger parameters are given in the Appendix.

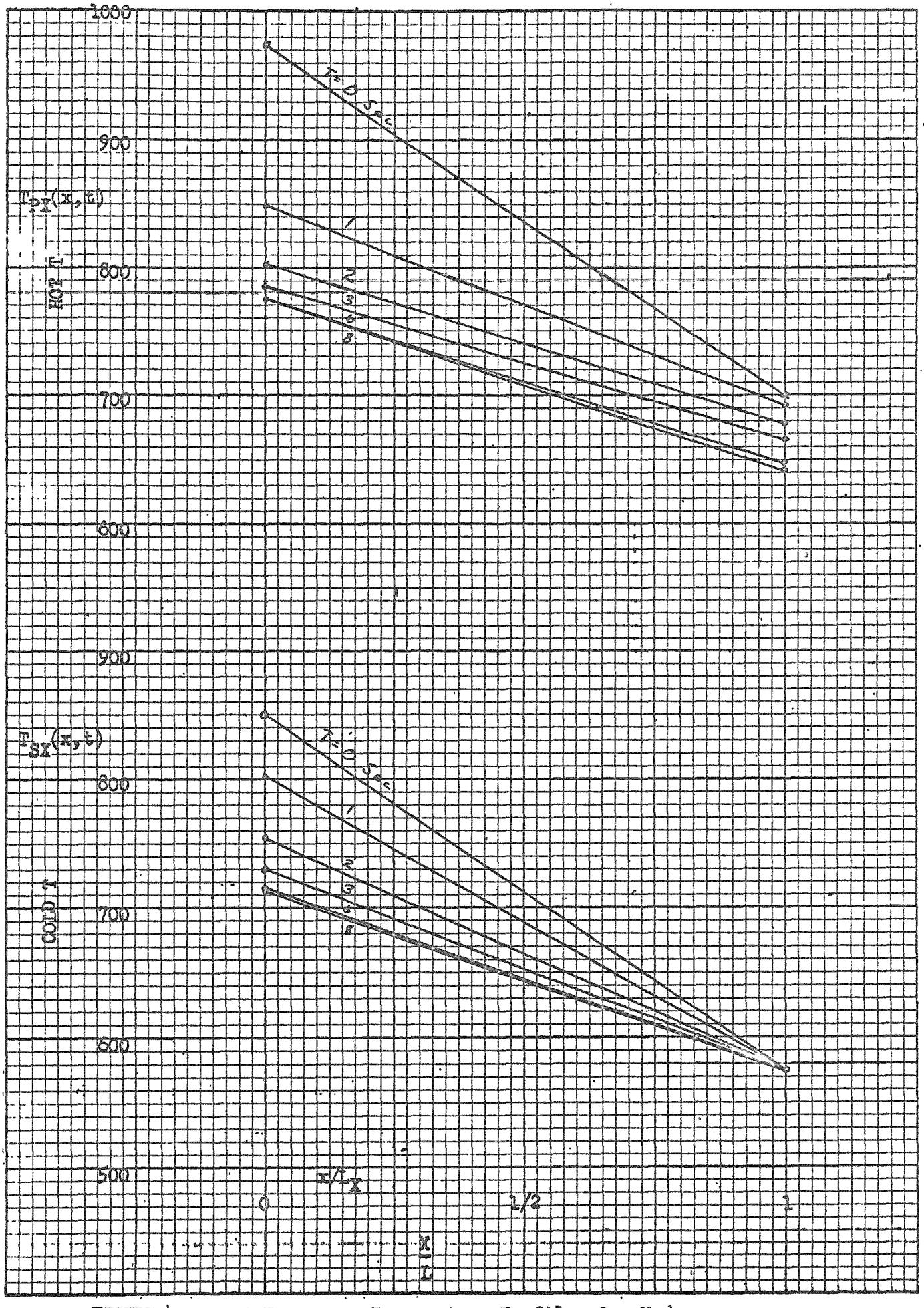

FIGURE 4. Heat Exchanger Temperature Profile, One Node

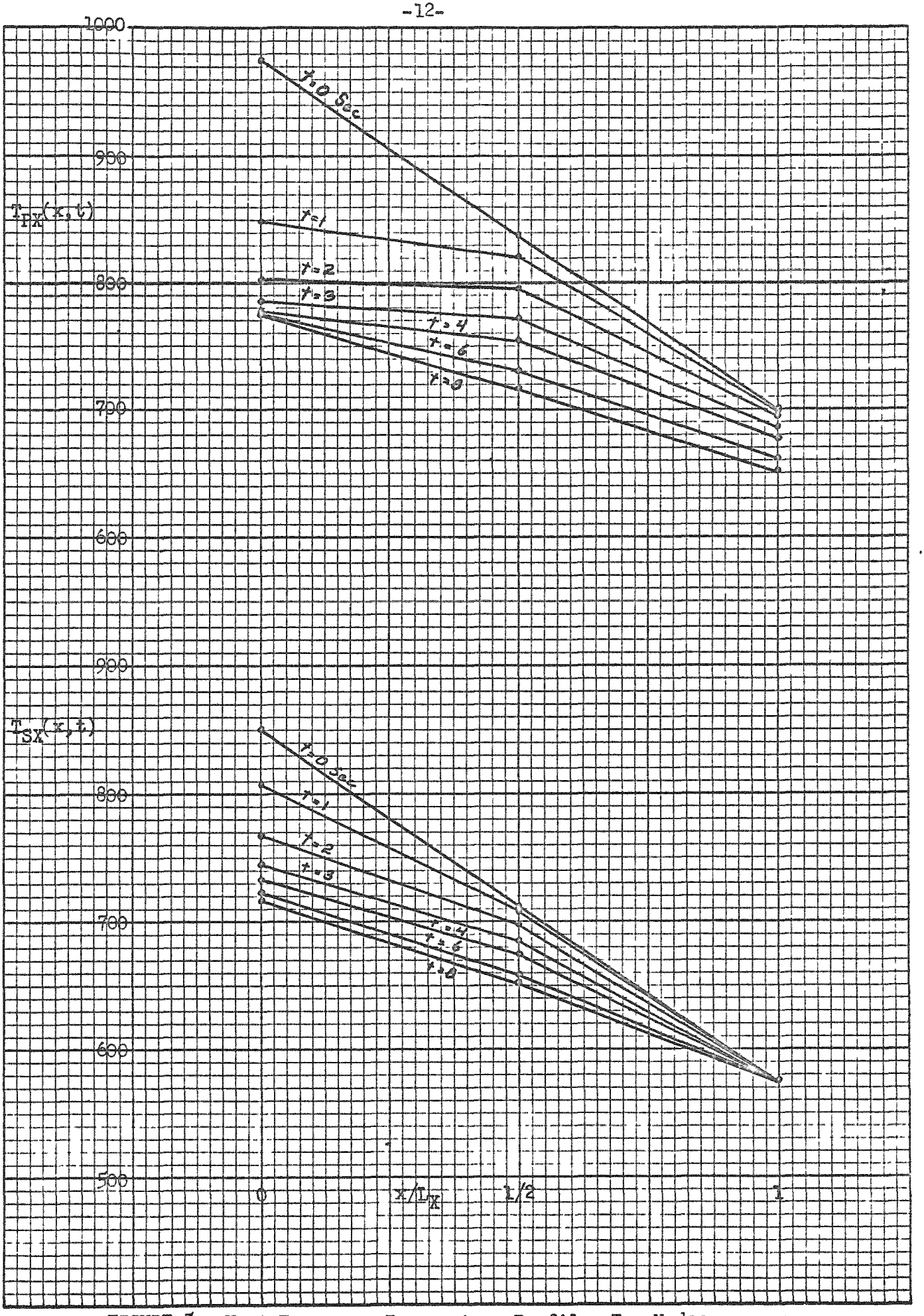

FIGURE 5. Heat Exchanger Temperature Profile, Two Nodes

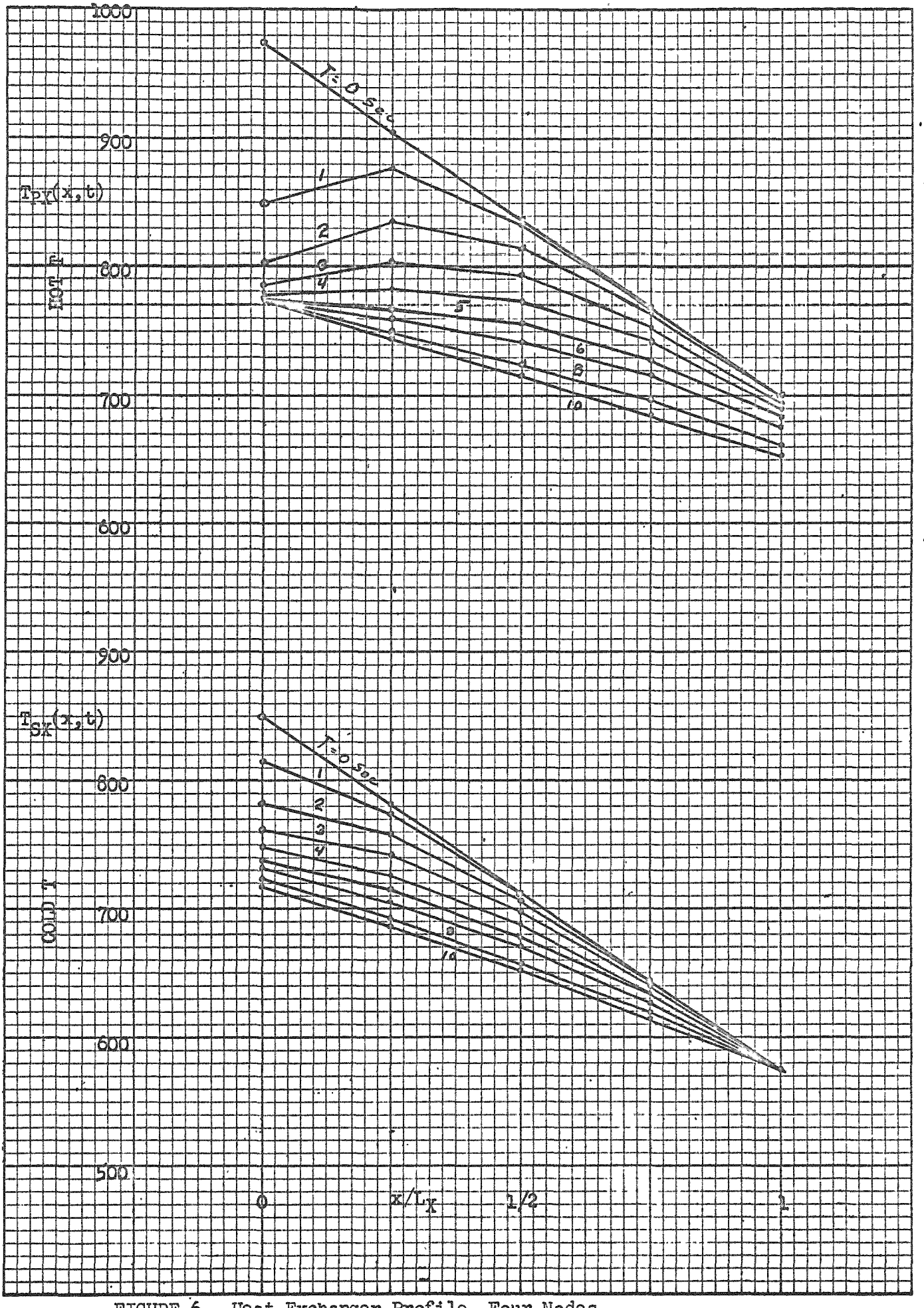

FIGURE 6. Heat Exchanger Profile, Four Nodes

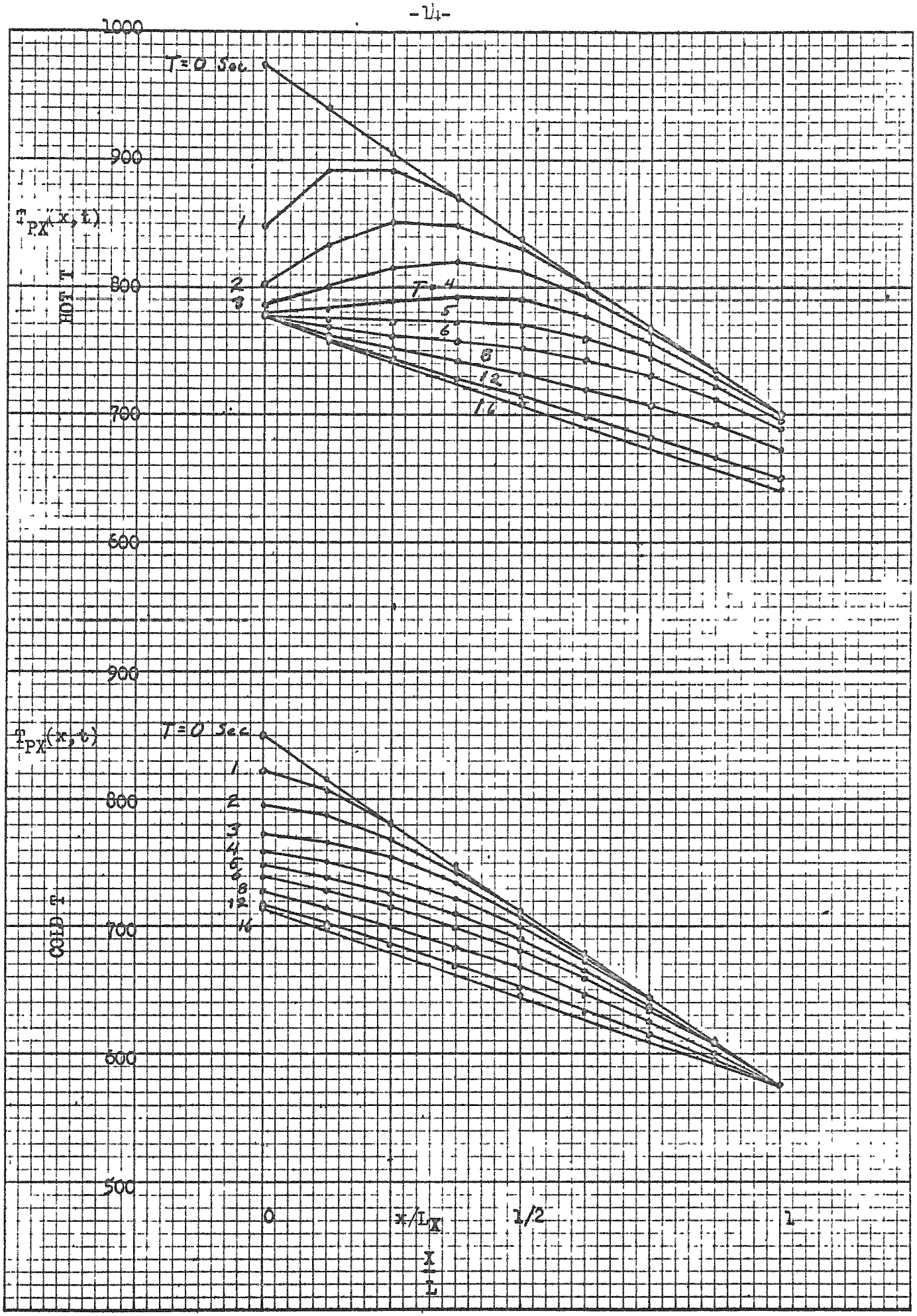

FIGURE 7. Heat Exchanger Profile, Eight Nodes

FIGURE 8

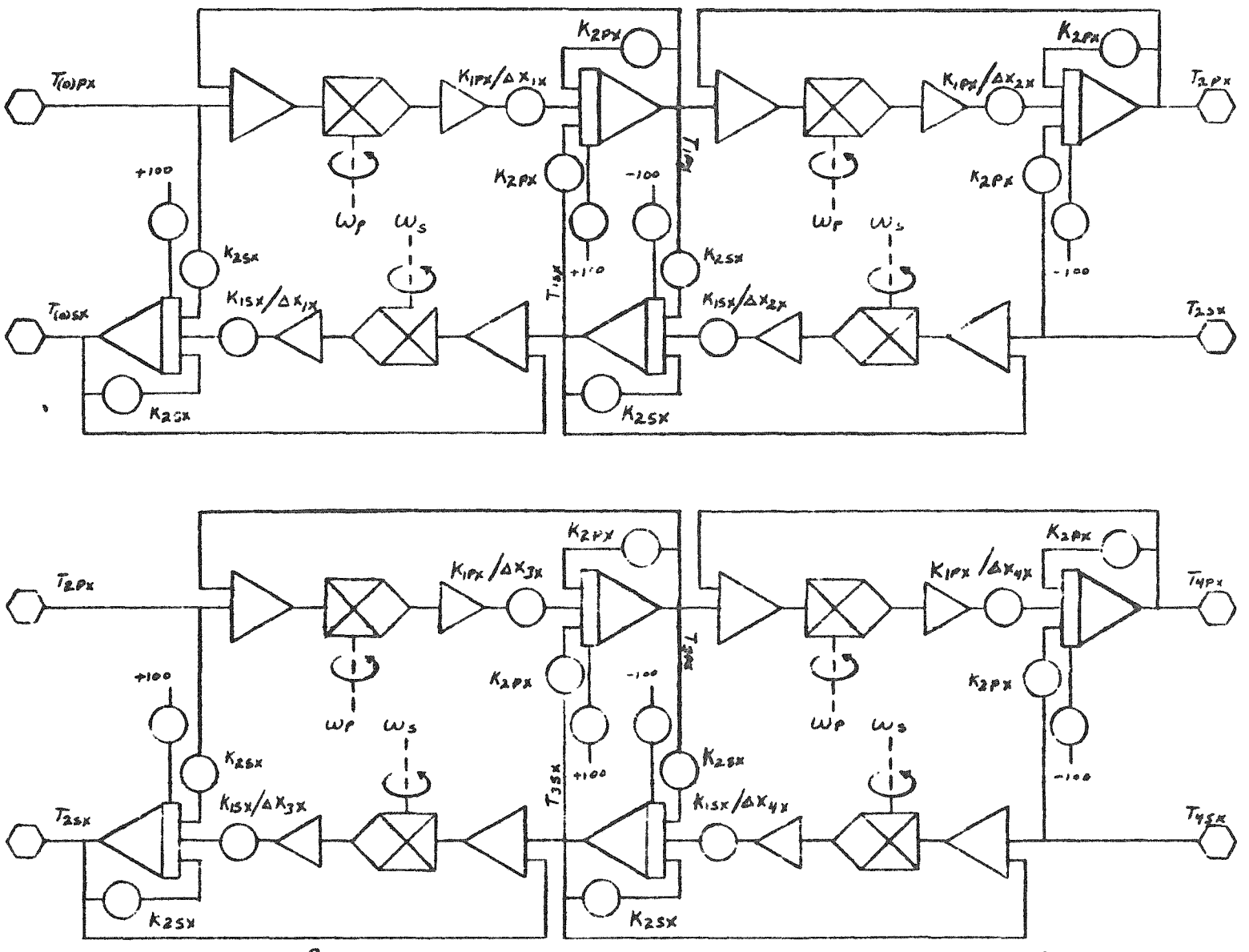

$$K_{1PX} = \frac{C_{CPX}}{A_{CPX}\rho_{CPX}C_{CPX} + A_{MPX}\rho_{MPX}C_{MPX}}$$

$$K_{1SX} = \frac{C_{CSX}}{A_{CSX}\rho_{CSX}C_{CSX} + A_{MSX}\rho_{MSX}C_{MSX}}$$

$$K_{2PX} \quad \frac{U_X A_X / L_X}{A_{CPX}\rho_{CPX}C_{CPX} + A_{MPX}\rho_{MPX}C_{MPX}}$$

$$K_{2SX} \quad \frac{U_X A_X / L_X}{A_{CSX}\rho_{CSX}C_{CSX} + A_{MSX}\rho_{MSX}C_{MSX}}$$

APPENDIX A

Calculation of Heat Exchanger Constants

The FFTF intermediate heat exchanger is to have 656 tubes, each 24 feet long arranged in a triangular pattern. The basic geometry is[3] shown in Figure 9.

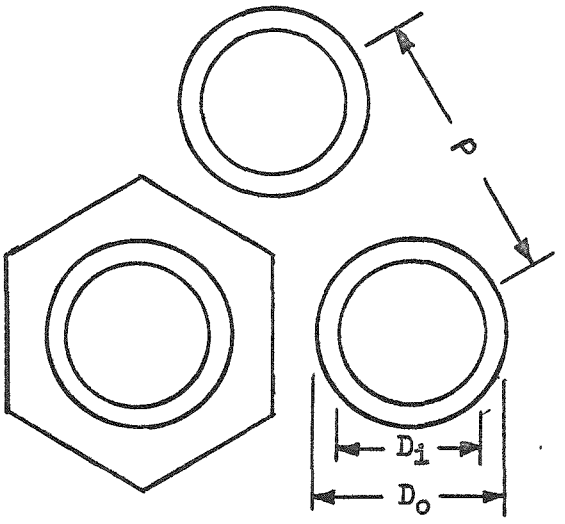

FIGURE 9

Intermediate Heat Exchanger Tube Geometry

The dimensions of the IHX[1] are:

Symbol	Quantity	Value
n_{TX}	Number of tubes in IHX	656
L_X	Tube length	24 ft
D_i	Tube inside diameter	.902 in.
D_o	Tube outside diameter	1.000 in.
P	Tube pitch	1.375 in.

The area of primary coolant flow (shell side) is:

$$A_{CPX} = n_{TX}\left[12(\tfrac{1}{2})\frac{P}{2\sqrt{3}}\left(\frac{P}{2}\right) - \frac{\pi}{4}D_o^2\right]$$

$$= \frac{n_{TX}}{4}\left[2\sqrt{3}\,P^2 - \pi D_o^2\right]$$

$$= 3.88 \text{ ft}^2$$

The area of secondary coolant flow (tube side) is:

$$A_{CSX} = \frac{n_{TX}\,\pi D_i^2}{4}$$

$$= 2.95 \text{ ft}^2$$

The cross sectional area of the tubes is:

$$A_{Tubes} = n_{TX}(\pi/4)(D_o^2 - D_i^2)$$

$$= n_{TX}(\pi/4)(D_o - D_i)(D_o + D_i)$$

$$= .665 \text{ ft}^2$$

The mass and specific heat of the tubes is lumped into the secondary side of of the exchanger.

$$A_{MSX} = 0.665 \text{ ft}^2$$

The heat transfer area is:

$$A_X = n_{TX}L_X\pi D_i$$

$$= 3720 \text{ ft}^2$$

The value of heat transfer coefficient to be used at design conditions can be obtained from:

$$\frac{w_P C_{CPX}}{L_X}\left(T_{(o)PX} - T_{(n_X)PX}\right) - \frac{U_X A_X}{L_X}\Delta T_{MX} = 0$$

where ΔT_{MX} is the log mean temperature difference (125 °F). Therefore,

$$\frac{U_X A_X}{L_X} = \frac{(2270 \text{ lb/sec})(.31 \text{ Btu/lb °F})(975 \text{ °F} - 700 \text{ °F})}{(24 \text{ ft})(125 \text{ °F})}$$

$$= 64.5 \text{ Btu/sec °F ft}$$

$$U_X = (64.5 \text{ Btu/sec °F ft}) \frac{6 \text{ ft}}{3720 \text{ ft}} = .104 \frac{\text{Btu}}{\text{sec °F ft}^2}$$

Sodium densities for primary and secondary sides are approximately 52.7 and 53.8 lb/ft^3, respectively. These values represent the densities at bulk design temperatures and are accurate to within ± 1.3 percent per 100 °F variation in temperature. The specific heat for sodium is 0.31 Btu/lb °F ± 3% for temperatures between 400 and 2000 °F. Therefore,

$$A_{CPX}\rho_{CPX}C_{CPX} = (3.88 \text{ ft}^2)(52.7 \text{ lb/ft}^3)(.305 \text{ Btu/lb-°F}) = 62.4 \text{ Btu/ft °F}$$

$$A_{MPX}\rho_{MPX}C_{MPX} = 0$$

$$A_{CSX}\rho_{CSX}C_{CSX} = (2.95 \text{ ft}^2)(53.8 \text{ lb/ft}^3)(.305 \text{ Btu/lb-°F}) = 48.8 \text{ Btu/ft °F}$$

$$A_{MSX}\rho_{MSX}C_{MSX} = (.665 \text{ ft}^2)(484 \text{ lb/ft}^3)(.12 \text{ Btu/lb-°F}) = 38.6 \text{ Btu/ft °F}$$

For uniform spacing of four nodes,

$$\Delta x_{KX} = L_X/n_X = 6.0 \text{ feet for all nodes.}$$

Bibliography

1. Progress Report Fast Flux Test Facility, Interim Reference Concept, BNWL-CC-400, Feb. 1966.

2. Swanson, C. D. Analog Simulation of a Preliminary FFTF Conceptual Design, BNWL-CC-381, Dec. 1965.

3. Johnson, H. G. FFTF Simulation, Appendix 2.

NOMENCLATURE

Symbol	Description	Value	Units
A_{CPX}	Area, cross section, coolant, primary	3.88	ft^2
A_{CSX}	Area, cross section, coolant, secondary	2.95	ft^2
A_{CSX}	Area, cross section, metal primary	0	ft^2
A_{MSX}	Area, cross section metal secondary	0.665	ft^2
A_X	Area, heat transfer surface	3720	ft^2
C_{CPX}	Specific heat, coolant, primary	.31	Btu/lb ^oF
C_{CSX}	Specific heat, coolant, secondary	.31	Btu/lb ^oF
C_{MPX}	Specific heat, metal, primary		Btu/lb ^oF
C_{MSX}	Specific heat, metal, secondary	.12	Btu/lb ^oF
L_X	Length, tubes	24	ft
M_{CPX}	Mass, coolant, primary		lb
M_{CSX}	Mass, coolant, secondary		lb
M_{MPX}	Mass, metal, primary		lb
M_{MSX}	Mass, metal, secondary		lb
n_X	Number of nodes in model	4	
n_{TX}	Number of tubes	656	
q	Heat transfer rate primary to secondary		Btu/sec
$\dot{Q}_P$	Heat storage rate, primary		Btu/sec
$\dot{Q}_S$	Heat storage rate, secondary		Btu/sec
$\dot{Q}_{Pin}$	Heat inlet rate to primary differential section		Btu/sec
$\dot{Q}_{Pout}$	Heat outlet rate from primary differential section		Btu/sec
$\dot{Q}_{Sin}$	Heat inlet rate to secondary differential section		Btu/sec

Symbol	Description	Value	Units
$\dot{Q}_{Sout}$	Heat outlet rate from secondary differential section		Btu/sec
t	time		sec
$T_{(K)PX}$	Temperature, K^{th} node, primary		^{o}F
$T_{(K)SX}$	Temperature, K^{th} node, secondary		^{o}F
$T_{PX}(x)$	Temperature, primary, as function of distance		^{o}F
$T_{SX}(x)$	Temperature, secondary, as function of distance		^{o}F
U_X	Heat transfer coefficient		$Btu/ft^2\text{-}sec\text{-}^{o}F$
w_P	Flow rate primary		lb/sec
w_S	Flow rate secondary		lb/sec
x	distance		ft
Δx_{KX}	Distance between node k-1 and node k	6	ft
ρ_{CPX}	Density, coolant, primary	52.7	lb/ft^3
ρ_{CSX}	Density, coolant, secondary	53.8	lb/ft^3
ρ_{MPX}	Density, metal, primary		lb/ft^3
ρ_{MSX}	Density, metal, secondary	484	lb/ft^3